Iranian Journal of Organic Chemistry Vol. 12, No. 1 (2020) 2771-2785

Mechanistic investigation of the [1+4] cycloaddition reaction between alkyl isocyanides and 3-benzylidene-2,4-pentanedione: A theoretical study

Mohammad Zakarianezhad*[a], BatoulMakiabadi[b], AtefehAbbaslou[a]

[a]*Department of Chemistry, Payame Noor University, Tehran, Iran*
[b]*Department of Chemical Engineering, Sirjan University of Technology, Sirjan, Iran*

Received: November 2019; Revised: December 2019; Accepted: January 2020

Abstract: The stepwise reaction mechanism of the [1+4] cycloaddition reaction between alkyl isocyanides (contains methyl benzene isocyanide, tert-butyl isocyanide, cyclohexyl isocyanide) with 3-Benzylidene-2,4-pentanedione both in the gas phase and in solvent was studied theoretically with B3LYP method using 6-311++G(d,p) basis set. The potential energy of all structures participated in the reaction path has been evaluated. The quantum mechanical calculation was performed to gain a better understanding of the most important geometrical parameters, determine the solvent effect, and the effect of different substituted groups on the potential energy surfaces. Unexpectedly, the second step of all reactions was recognized as the rate-determining step. The best product configuration was recognized based upon the quantum mechanical calculations. The natural bond orbital method (NBO) applied for a better understanding of molecular interaction.The final rate equation shows that the overal reaction rate is second order which depends on the R1 and R2 concentration. The order of reaction with respect to each reactant is one.

Keywords: Theoretical study, Alkyl isocyanides, [1+4] cycloaddition, Reaction mechanism

Introduction

In recent years, the design of multicomponent reactions (MCRs) that preserve atom economy, conversion character, and simplicity in a one-pot operation has received considerable interest due to their ability to generate highly complex final products [1]. These reactions emerge as an efficient construction in the synthesis of drug libraries because they have significant advantages over conventional reaction strategies to generate biologically actives caffolds with significant structural diversity. In particular, isocyanide based multicomponent reactions (IMCR) have acquired a major position in this field. IMCRs are fast and selective techniques for the synthesis of complex structures and diverse chemical libraries of drug-like molecules [2].

Isocyanides compounds are important materials in chemistry and many of them have found general application in organic synthesis. An isocyanide (also called isonitrile or carbyl amine) is an organic compound with the functional group -N≡C. The organic fragment is connected to the isocyanide group via the nitrogen atom, not via the carbon. Alkyl isocyanides are used as the important mediate in the synthesis of a wide range of compounds. Isocyanides are reactants in many multicomponent reactions of interest in organic synthesis, two of which are: the Ugi reaction [3] and the Passerini reaction [4]. Furans are one of the most important compounds in organic and synthetic organic chemistry. Many of furan products show inspiring biological activities, such as cytotoxic and antitumor properties, antispasmodic, antifeeding, and antimicrobial activities [5]. Polysubstituted furans are important precursors for the synthesis of natural and no natural products. The synthetic efforts towards

*Corresponding author: Tel: +983442335743, E-mail: m.zakarianejad@yahoo.com

polysubstituted furans belong therefore to an exceedingly active research domain. Polysubstituted furans, various annulated derivatives such as benzo, thieno,isoxazolo, furo, pyridino, pyridazino, and indolofuran have been synthesized and their properties investigated [6].Furans are useful synthetic intermediates [7-9] finding utility asmasked a,b-unsaturated esters [10] and as precursors to hydroxypyranones 11] and polyoxygenated natural products [12] as well as two mono and oligosaccharides. Furan substructures are an important motif in materials chemistry providing promising plastics derived from renewable sources [13], self-healing macromolecular materials [14], conducting polymers [15], and photovoltaics [16] Hence, the synthesis of furans has attracted considerable attention [17,18]. Isocyanides undergo a formal [1+4] cycloaddition reaction with conjugated electrophilic heterocyclic five-membered ring systems [19].In this reaction, after the formation of a zwitterionic intermediate, the final product produced via a stepwise [1+4] cycloaddition. The quantum mechanical calculation was performed to gain a better understanding of the most important geometrical parameters. Also, to determine different parameters affecting the reaction mechanism and determining the effect of different substituted groups on the potential energy surfaces, the reaction mechanism was evaluated in detail.

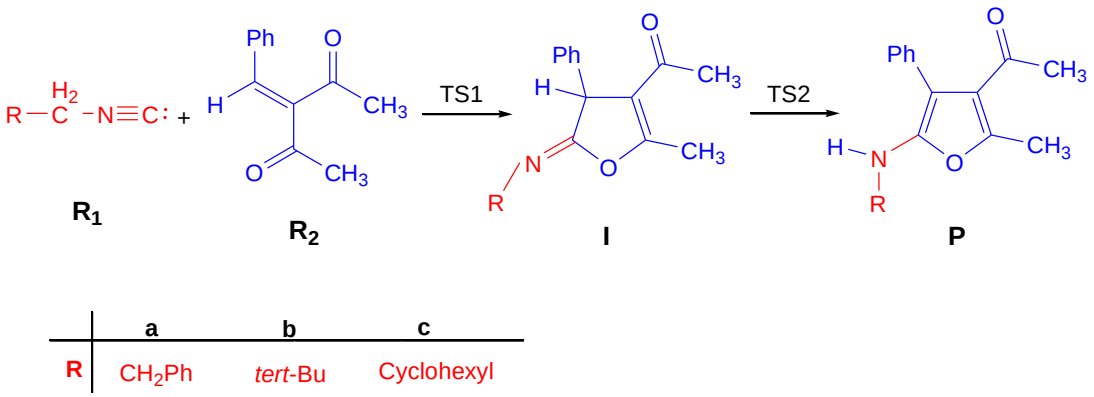

Figure 1: The Reaction between alkyl isocyanides (**R1-a**,**R1-b,** and **R1-c**) with 3-Benzylidene-2,4-pentanedione (**R2**).

Result and Discussion

Energetics and geometries in the gas phase and solution:

Alkyl isocyanides (R1) with different substituted alkyl groups include methyl benzen isocyanide (R1-a), tert-butyl isocyanide(R1-b) and cyclohexyl isocyanide (in two forms; boat (R1-c1) and chair (R1-c2)) react with 3-benzylidene2,4-pentan dione (R2).Three different pathways (a, b, c1(c2)) were predicted in this reaction. The optimized geometries of all structures are presented in Figs. 2 and 3.Also, Potential energy profiles for all pathways are presented in Fig.4.In the first step of the reaction, atom C14 of R2was attacked by atom C27 of alkyl isocyanides (R1), as a nucleophile atom, and I1 (I-a, I-b, I-c1, and I-c2) produced via passing Ts1 (Ts1-a, Ts1-b, Ts1-c1, and Ts1-c2). In the second step of the reaction, the product, P (P-a,P-b,P-c1,and P-c2) produced via a proton transfer from C14 to N28 and passing from Ts2. Because of the orientation of the phenyl group in the structure of methyl benzene isocyanide (R1-a), the first step of the reaction proceeds via two competitive paths a and a‘ with the energy barriers of 91.0 and 93.3 kJ/mol, respectively. The barrier height of the path a is less than the path a‘ by 2.3 kJ/mol. The second step of the reaction, with the barrier energy of 298.4 kJ/mol, proceeds very slowly. Negative values of ΔH (-114.1kJ/mol) and ΔG (-55.2 kJ/mol) indicate that the reaction is exothermic and spontaneous. In the presence of di-tert-butyl isocyanide (R1-b), the second step of the reaction was also recognized as the rate-determining step. The second step barrier energy of the reaction (285.2kJ/mol) is also considerably higher than the first step of the reaction (91.3 kJ/mol). Negative values of ΔH (-93.6 kJ/mol) and ΔG (-33.1 kJ/mol) indicate that the reaction in this pathway is exothermic and spontaneous. The barrier energies of the second step of the reaction in the presence of R1c1 and R1c2are 292.4 and 292.8 kJ/mol, which are almost the same and not much different. These barrier heights are also considerably more than the first steps (92.8 and 93.9 kJ/mol, respectively).These

two paths because of the same reactant, product, and the same barrier heights, have no kinetic or thermodynamic preference over each other. The path a with leading to the most stable product (P-a), was recognized as a thermodynamically preferred route. Also, the path b with the least barrier height was recognized as a kinetically preferred route. The potential energy of Ts1-a(Ts1-a'),Ts1-b,andTS1-c1 (TS1-c2)indicate that different substituted groups in the structure of R1 didn't make significant changes in the potential energy of the first step of the reaction path. The potential energy of Ts2-a, Ts2-b, and TS2-c1 (TS2-c2)is 199.4 kJ/mol, 206.5 kJ/mol, and 200.6 (201.2 kJ/mol), respectively, and indicates a significant effect of substituted groups in the structure of R1.The potential energy of P-ais -110.2 kJ/mol which is more stable than P-b(-94.7 kJ/mol). Products P-c1 (P-c2) with the potential energy of -103.1 (-103.6 kJ/mol) have no thermodynamic preference towards each other but are more stable than P-b. P-a is the most stable product. So, the path a is the most thermodynamically stable one which initiates with the reactant of R1-a.Evaluation of the potential energy surfaces in the second step of the reaction mechanism (proton transfer step) shows that the stability sequence of the energy levels of the reactants, the transition state, and the product is equal to a>c1≈c2<b. The result shows that the transition state structures in more stable structures have lower energy levels, while, the proton transfer energy barrier is more, in more stable structures. This result is because of the greater stability of intermediate (I) in these structures.

To investigate the effect of solvent on the potential energy surfaces, all the structures were optimized in the solution phase and the presence of the two solvents of acetone and dichloromethane with the dielectric constants of 20.49 and 8.93, respectively. The results show that the potential energy level of the transition states in the first and second steps has increased substantially in comparison with the gas phase, but the potential energy level of the reactants, intermediates, and products has been more stable in comparison with the gas phase. So, the energy barrier has increased dramatically in comparison with the gas phase. The barrier height of the first step of the path a)a´) in acetone is equal to 181.1 kJ/mol (182 kJ/mol). This energy barrier in dichloromethane is equal to 181.3 kJ/mol (182.5 kJ/mol) which shows slight changes in the energy barrier. In acetone solvent, the energy barrier of the second step of the reaction in the presence of R1-a is equal to 614.5 kJ/mol that in comparison with the energy barrier of the first step, has increased to the amount of 433.4 kJ/mol (432.06 kJ/mol). Also, in thedichloromethane solvent, the energy barrier of the second step of the reaction is 614.7 kJ/mol that has increased substantially, compared with the energy barrier of the first step. The energy barrier of the first step of the patha(a´) in acetone is less stable than the gas phase by the amount of 90.1 kJ/mol (88.7 kJ/mol) and also in dichloromethane it has become less stable by the amount of 90.3 kJ/mol (89.2 kJ/mol).

In comparison with the gas phase, the energy barrier of the second step of this reaction in acetone and dichloromethane solvents are 316.1 kJ/mol and 316.3 kJ/mol and this amount shows the substantial growth of the energy barrier as compared to the first step. The overall results show that the effects of solvent dielectric constant on the energy barrier of the first and second steps are negligible. It means that in dichloromethane and acetone, there isn't any specific difference in the energy barriers of the first and second steps.

The energy barrier of the first and second steps of the reaction mechanism in the presence of R1-band acetone are 180.1 and 593.5kJ/mol, respectively, which shows a significant increase of the second step barrier compared to the first step of reaction mechanism by 413.4kJ/mol. The energy barrier in first and second steps of reaction mechanism in the presence of R1-b in dichloromethane, are 180.6 and 592.5 kJ/mol and show its significant increase compared to the first step of the reaction mechanism by 411.9kJ/mol. The energy barrier of the first step of the reaction in acetone and dichloromethane solvents comparing to the gas phase had increased by 88.8 kJ/mol and 89.3 kJ/mol, respectively. Energy barrier in the second step of this reaction in acetone and dichloromethane solvents comparing to the gas phase had increased, respectively, by 308.3kJ/mol and 307.3 kJ/mol. The energy barrier of the second step of the reaction in the presence of R1-c1 (R1-c2) in acetone solvent is 607.9kJ/mol (608.2kJ/mol). However, in comparison to the energy barrier of the first step, it increased by 426.2kJ/mol (425.5kJ/mol). In dichloromethane also energy barrier of the second step increased compared to the first step. The amount of increase is 424.9 kJ/mol (419.4 kJ/mol). The energy barrier in the first step of this reaction in acetone compared to the gas phase, increased by 88.9kJ/mol (88.8kJ/mol) and the energy barrier of the second step comparing to gas phase increased by 315.5kJ/mol (315.4kJ/mol). The energy barrier in the first step of this reaction in the dichloromethane solvent increased compared to the gas phase by 892kJ/mol (88.4kJ/mol).The energy barrier of the second step, compared to the gas phase, also increased by 314.5kJ/mol (308.9kJ/mol).

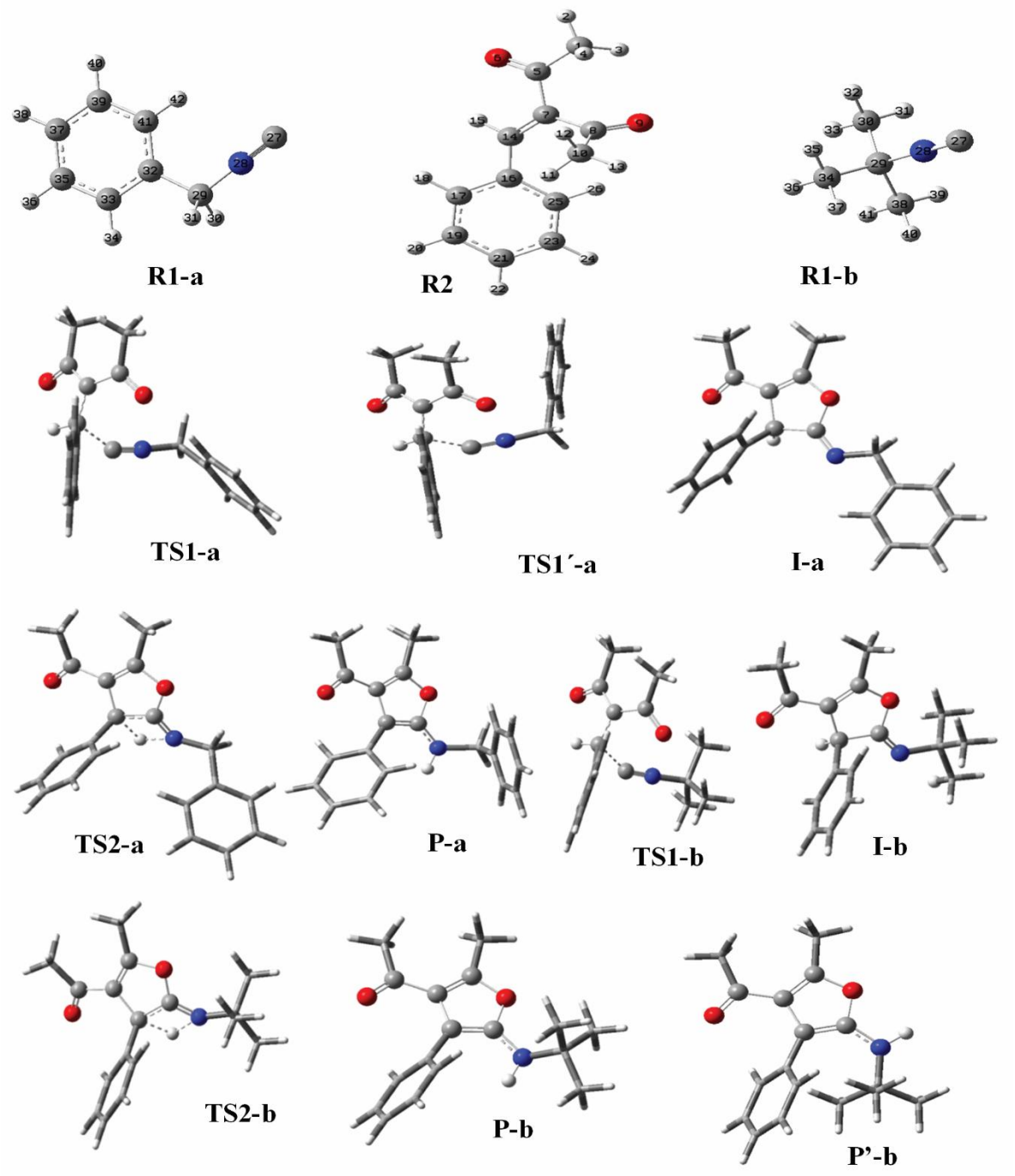

Figure 2: Optimized geometries of all structures in the pathways **a** and **b**at B3LYP/6-311++g(2d,2P) level of theory.

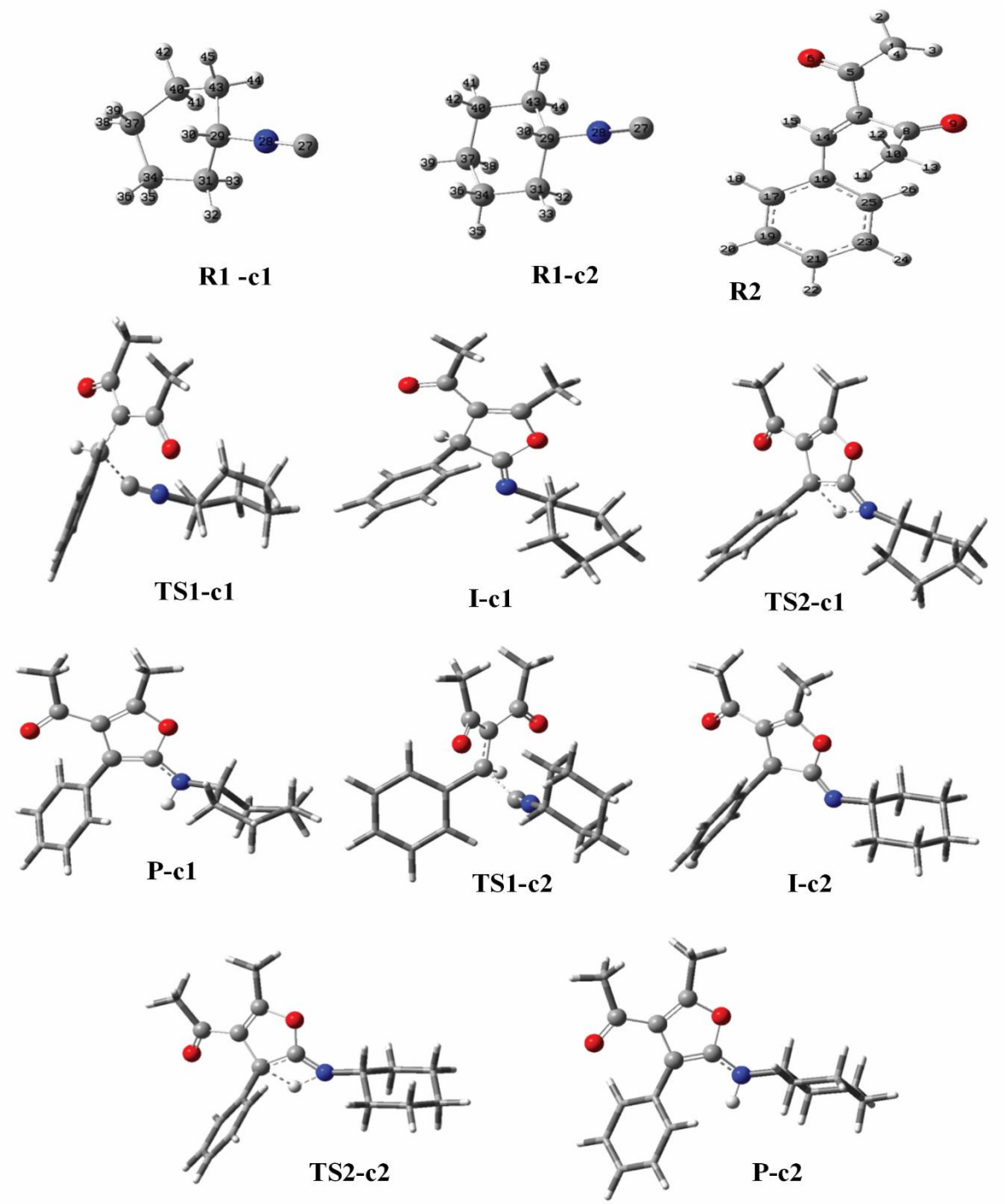

Figure 3: Optimized geometries of all structures in the pathways c1(c2)at B3LYP/6-311++g(2d,2P) level of theory.

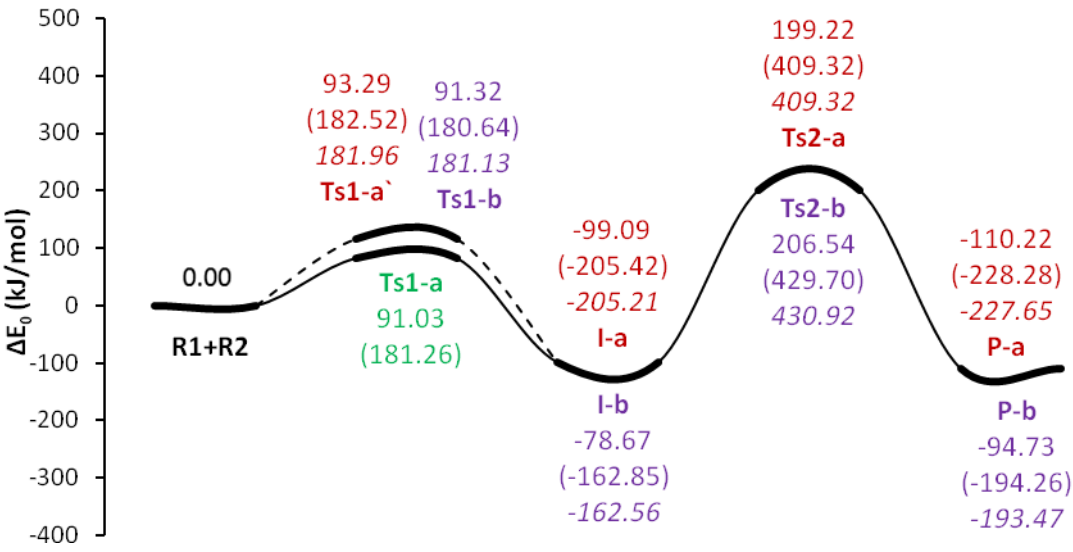

Figure 4: The potential energy profile of the reaction in paths **a** and **b**(data in dichloromethane are in parentheses and data in acetone are in italic form.

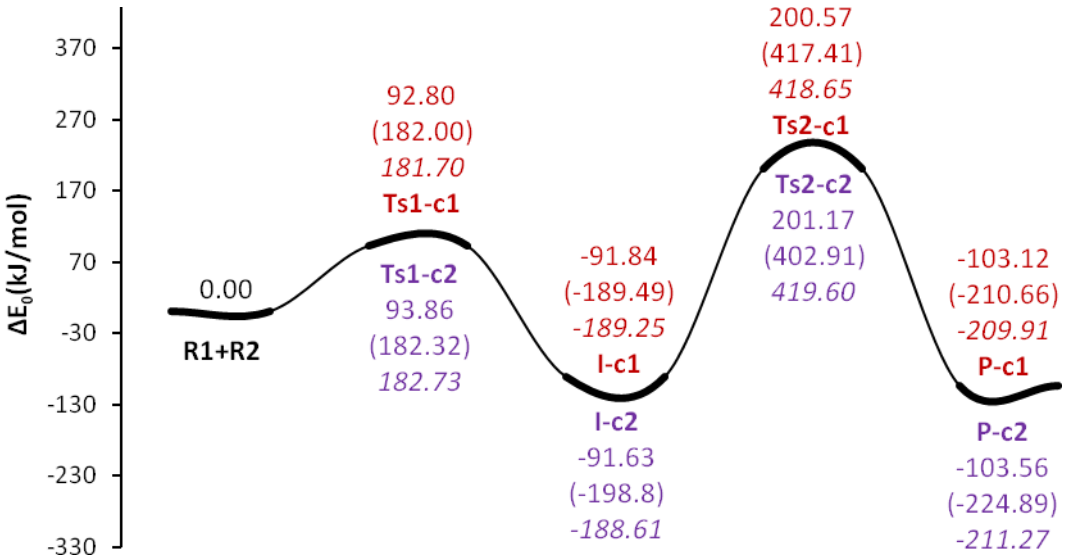

Figure 5: The potential energy profile of the reaction in paths **c1** and **c2** (data in dichloromethane are in parentheses and data in acetone are in italic form.

A comparison of findings among the structures of transition state shows that the most stability in solution phase is related to TS1-b. These results can be due to the presence of concentrated charge in transition state structure. The amount of negative and positive charge in Ts1-b can be more than other transition state structures. In NBO analysis section, we'll talk more in details. Increase or decrease of energy barrier in solution phase is dependent on the amount of stability of the transition state and reactants. Results show that in the presence of acetone, the energy barrier of structures participating in the reaction mechanism decreased compared to dichloromethane. Relative enthalpy (ΔH) and relative Gibbs free energy (ΔG) in both solvents show that in each of the mechanisms, the reaction is exothermic and spontaneous.

But the reaction is more exothermic and spontaneous in the path a. In the presence of both solvents, path b has also kinetic preference. More analysis shows that although the energy barrier of first and second step in the presence of solvents (acetone and dichloromethane) has significantly increased, but the amount of changes in both acetone and dichloromethane is approximately equal. More details showed that the energy level of TS1-a comparing to TS1-a´,in each mechanism, is slightly more stable in the presence of both acetone and dichloromethane, but in comparison with the gas phase, this energy level has significantly increased and is more unstable. The energy levels ofTS1-b, TS1-c1 and TS1-c2in acetone is also more stable than in dichloromethane, but compared to the gas phase, this energy level has significantly increased. The energy levels of intermediates I-a, I-b, I-c1 and I-c2 in acetone and dichloromethane are very close to but in comparing with gas phase shows a significant increase. In the intermediates, the most stable energy level corresponds to I-a. The energy level of the second step in transition state shows a significant increase compared to gas phase. The most stable energy level in the transition state of the second step in gas phase and in acetone belongs to TS2-a and the most stable energy level in dichloromethane solvent belongs to TS2-c2. The potential energy surfaces of products P-a, P-b, P-c1 andP-c2 in solvents also significantly increased compared to gas phase. The energy level of the most stable products in the presence of solvents and also in gas phase corresponds to P-a. On the whole, it can be said that all the structures in acetone solvent are more stable comparing to dichloromethane. Results indicated that the amount of change in potential energy levels in both acetone and dichloromethane, with different dielectric constant, had approximately been equal.

Dipole moment values (μ) concerning the structure involved in the reaction mechanism in gas phase and in the presence of dichloromethane and acetone had been depicted in Table **1**.In solution phase, by increasing the value of the dipole moment, solvent-soluble interaction increases and finally causes the structure to be more stable. The analysis of the results indicates that in acetone and dichloromethane, the amount of increase in dipole moment is approximately equal. The analysis of results (Table **2**) shows that by closingR1 to R2, the C27-N28 bond length and also the N28-C29bond length gradually increased. The amount of change in the bond length of C27-N28 is more than N28-C29.The bond length of C…N in the structure of R1-b increased compared to R1-a and then decreased in the structure of R1-c1 (R1-c2). In the structure of TS1, the most bond length of C…C interaction corresponds to the structure ofTS1-b and the least bond length corresponds to the structures of TS1-a and TS1-c1. In the intermediate I, the C14-C27 bond length is identical in the structures of I-a, I-b and I-c1 (I-c2). The bond length of C27-09 was identical in the structures of I-a and I-c1 (I-c2), but increased in I-b. In the structure of TS2, while transferring of H15 from C14 to N28, the bond length of C14-C27 decreased and C27-N28 bond length increased. The most increase of the bond length of C27-N28 and the most decrease is in the bond length of C14-C27 corresponds to P-a. In the final product (P), as same as TS2, the changing procedures of the bonds of C14-C27 and C27-N28 in the presence of reactantsR1-a, R1-b, R1-c1 and R1-c2are the same.

The analysis of natural bond orbital (NBO) and atoms in molecule (AIM):

The NBO analysis, including charge transfer energy and atomic charges, will give us a better understanding of the interactions. Also, to achieve a deeper sight about the nature and strength of hydrogen bonds, electron density analysis at bond critical points ρ(r), laplacian electron density at bond critical points (ρ(r)), the total electron density H(r), the density of electronic kinetic energy G(r), at bond critical points (BCPs) was calculated using the theory of atoms in molecules (AIM)at B3LYP/6-311++G(2d,2P) level of theory. The charge analysis of the atoms participant in the reaction mechanism and important electrontransfers in the gas phase at the B3LYP/6-311++G(2d,2P) level, are reported in Table **3**. The structure of TS1-a, resulting from a nucleophilic attack of atom C27 to atom C14. NBO analysis indicated that in this nucleophilic attack, a charge transfer occurs from R2 to R1-aby the value of 0.348e.

Table 1: Dipole moment values (μ/D) of all structures participating in the reaction mechanism both in the gas phase and in solution.

structure	Gas-phase	acetone	dichloromethane	structure	Gas-phase	acetone	dichloromethane
R1-a	3.85	4.79	4.69	**R1-c1**	4.51	5.52	5.43
R2	4.00	5.00	5.00	**R2**	4.00	5.09	5.00
TS1-a	3.93	4.81	4.71	**TS1-c1**	4.69	5.58	5.50
TS1-a`	4.04	5.01	4.95	**I-c1**	4.10	6.22	5.91
I-a	4.28	6.34	6.05	**TS2-c1**	4.40	6.60	6.29
TS2-a	4.12	6.42	6.07	**P-c1**	4.098	5.68	5.45
P-a	3.46	4.79	4.58				
R1-b	4.14	5.21	5.10	**R1-c2**	4.50	5.52	5.39
R2	4.00	5.09	5.00	**R2**	4.00	5.10	5.00
TS1-b	4.33	5.35	5.23	**TS1-c2**	4.76	5.61	5.54
I-b	4.13	6.27	5.97	**I-c2**	4.11	6.24	5.93
TS2-b	4.34	6.53	6.22	**TS2-c2**	4.39	6.63	6.32
P-b	3.56	5.06	4.87	**P-c2**	4.12	5.69	5.49

Table 2: The important bond length of the structures in the gas phase at B3LYP/6-311++g(2d,2P) level of theory.

Structure	C_7-C_8	C_8-O_9	C_7-C_{14}	C_{14}-C_{27}	C_{27}-O_9	C_{27}-N_{28}	N_{28}-C_{29}	C_{14}-H_{15}	N_{28}-H_{15}
R1-a						1.17	1.42		
R2	1.50	1.21	1.35					1.09	
Ts1-a	1.46	1.23	1.41	1.94	3.08	1.16	1.43	1.08	3.41
Ts1`-a	1.46	1.23	1.42	1.93	3.05	1.16	1.44	1.08	3.44
I-a	1.35	1.38	1.52	1.52	1.41	1.25	1.46	1.09	2.83
Ts2-a	1.36	1.41	1.50	1.43	1.35	1.30	1.46	1.53	1.37
P-a	1.37	1.37	1.46	1.36	1.37	1.38	1.48	2.66	1.01
R1-b						1.17	1.45		
R2	1.50	1.21	1.35					1.09	
Ts1-b	1.46	1.23	1.42	1.95	3.57	1.16	1.45	1.08	3.43
I-b	1.35	1.38	1.52	1.52	1.42	1.24	1.48	1.09	2.80
Ts2-b	1.36	1.41	1.50	1.43	1.36	1.30	1.48	1.51	1.38
P-b	1.37	1.37	1.46	1.36	1.37	1.38	1.49	2.62	1.01
R1-c1						1.17	1.43		
R2	1.50	1.21	1.35					1.09	
Ts1-c1	1.46	1.23	1.41	1.95	3.53	1.16	1.43	1.08	3.42
I-c1	1.35	1.37	1.52	1.52	1.41	1.25	1.46	1.09	2.82
Ts2-c1	1.36	1.41	1.50	1.43	1.35	1.30	1.46	1.52	1.38
P-c1	1.37	1.37	1.46	1.36	1.37	1.38	1.47	2.67	1.01
R1-c2						1.17	1.43		
R2	1.50	1.21	1.35					1.09	
Ts1-c2	1.46	1.23	1.42	1.95	3.08	1.16	1.44	1.08	3.43
I-c2	1.35	1.37	1.52	1.52	1.41	1.25	1.46	1.09	2.82
Ts2-c2	1.36	1.41	1.50	1.43	1.36	1.30	1.46	1.52	1.38
P-c2	1.37	1.37	1.46	1.36	1.37	1.38	1.47	2.67	1.01

The charge density of atom C27 decreased from 0.270e to 0.455e. The charge of atoms C7 and C14 at TS1-aare -0.085e and -0.217e, respectively, which shows an increase in the amount of 0.116e and 0.008e.The charge of the atom O9 also increased from -0.557e to -0.645e. In this neocliphilic attack, it's been expected for the bond length of C7…C14 to be increased. Results from Table **2** indicate that the bond length increased by an amount of 0.06 Å. The bond length of C7-C8 decreased from 1.50 to 0.46 Å. With decreasing the density charge of atom C27, the atomic charge of N28 also decreased from -0.524e to -

0.402e.Decreasing the charge of C7 is the result of charge focusing on the C7-C8 bond. With the approaching of atom C27 to C14 and formation of covalent bonds in I-a, the negative charge of C14 was significantly increased (-0.296e), but the negative charge of atom C7 decreased by 0.140e. By decreasing the electronic charge of C27, the electronic charge of N28 was decreased from -0.402e to -0.486e. Therefore, as expected, the bond length of C-N increased from the amount of 1.16Å, in TS1-a, to the amount of 1.25Å, in I-a. Although the atomic charge of O9 increased in TS1-a, but in I-a, because it shared in O9-C27, decreased to its primary amount in R2. The atomic charge of N28 in R1-ais equal to -0.524e, whereas, its amount in R1-b and R1-c1 (R1-c2) is equal to -0.527e. Also, the positive charge of atom C27 in R1-b and R1-c1 (R1-c2) significantly decreased from 0.270e to 0.275e. Results indicate that in going fromR1-a to R1-b or R1-c1 (R1-c2), decreasing the positive charge of C27 is not due to an increase of the electron-withdrawing of N28.Because otherwise, increase of the negative charge of N28 in going fromR1-a to R1-b or R1-c1 (R1-c2),the positive charge of C27 leading to decreased. Thus, the increase of the negative charge of N28 and decrease the positive charge of C27 is the result of increasing the electron donation of substituted groups of tert-butyl or cyclohexyl. It is expected that atom C27 in R1-b and R1-c1 (R1-c2) with a higher electron density thanR1-a, have a more efficient nucleophilic attack to C14 atom. This efficient nucleophilic attack can decrease C14 -C27 bond length and also causes the activation energy barrier to be decreased. Analyses show that not only this bond length in TS1-b and TS1-c1 (TS1-c2) does not decrease, but also slightly increases. Results of AIM analysis (Table **4**) also show a decrease in the electronic density of this bond in TS1-b and TS1-c1 (TS1-c2) structure comparing to TS1-a. Also, the activation energy barrier, unexpectedly, increased. Results indicated that strict factor and the orientation of substituted groups will have a more effective role in changing structural parameters and decreasing the activation energy barrier.A comparison of both TS1-a with TS1′-a revealed that the C14-C27 bond length and also the energy barriers are not identical in these structures. This result also signifies the importance of the configuration. As it was mentioned, increasing the atomic charge of N28 with the value of -0.524e in R1-ato the value of -0.527e in R1-b or R1-c1 (R1-c2) can be the result of electron donation of the substituent groups or because of their higher strict factor. The strict factor and increasing of the N28-C29 bond length, can increase the polarity of this bond and consequently caused the electronic charge density of N28 to be increased. The bond length of N28-C29 confirms increasing of this bond length in R1-b and R1-c1 (R1-c2) in comparison with R1-a. It should be noted that the most increase in bond length of N28-C29 is related to R1-b. Analysis of I-a, I-b, I-c1 (I-c2) reveals that N28-C29 bond length in these structures is, 1.456, 1.477 and 1.460 (1.461Aº), respectively. The most bond length corresponds to I-b structure. The atomic charge of N28 in these structures is -0.486,-0.492 and -0.477 (-0.478e), respectively. At this time, also the most electronic charge belongs to the atom N28 at I-b structure. Electron density of bond critical points is also in accordance with the achieved results. More detailed results show that the amount of electronic charge changes in N28 and also the amount of changes of bond length and electron density of N28-C29 are more than R1-a, R1-b and R1-c1 (R1-c2).It is expected that the presence of identical substituted groups with an equal electron donating at the structures ofR1 and I show the same electronic effects, but results show different behavior of them inR1 and I structures. Results also better show the strict effect of more bulky substituted groups of b, c1 (c2) compared to the a substituted group. Because in bulky structures of I-a, I-b, I-c1 (I-c2), the strict effect will demonstrate its more tangible effect on the structural parameters and electronic properties. These changes in the bulkier structure of I-bare more than other structures, because the substituent group b in this structure can impose more strict effect. It is expected that the increase of N28 –C29 bond length be associated with increase of N28 atomic charge. More detailed results show that the changes of the bond length at I-a, I-b, I-c1 (I-c2), in some cases, is not compatible with the changes of the atomic charge of N28. This can be the result of atomic charge changes of C27connected to N28 at the structure of I. The atomic charge of this atom inR1 is identical, but in I structures, some changes in the charge of this atom were observed. Since R2 is identical in all the structures, the source of changes in the electronic charge of this atom is the substituted groups of a, b, c1(c2) in the structure of R1. Based on these results, it is expected that bond lengths of C27-O9 and C27-C14 also experienced some changes. Results indicate that the length of these bonds in bulky structures of I-b, I-c1 (I-c2) in comparison with I-a, has increased. This time, too, the most changes of the bond length correspond to I-b. The positive charge of C27 in intermediate structures (I) compared to R1 has significantly increased. Decreasing the charge density of C27 is related to loss of electron density in nucleophilic attack to C14 atom. Increasing the negative charge of

C14 in R2 from -0.085e to -0.296e also confirms this fact. However, negative charge of O9 in R2 and I structures didn't have any significant change. The negative charge of N28 in R1 structures was decreased, in comparison with I structures. Decreasing the negative charge of N28 atom can be as a result of two important interactions including LPN28→BD* O9-C27 and LPN28→BD* C14-C27 at I structures. There is no special relationship between the electron density of C14–C27 bond at the structures of TS1-a, TS1-b and TS1-c1 (TS1-c2) and the atomic charge of C27 at R1-a, R1-b and R1-c1 (R1-c2) structures. This can be due to the complicated effects of strict effect and electron donation or electron affinity of the substituted groups. In the structures of I-a, I-b andI-c1 (I-c2), such a manner have also been observed. The second step of the reaction mechanism includes the transition of atom H15 from C14 to N28. In this process, the structure I, after passing from transition state TS2, coverts to the final product (P). Based on the reaction potential energy diagram (Fig. 4), although the final product comparing the intermediate structure will have thermodynamic stability, but it must pass a significant energy barrier. During the proton transfer process, by the formation of the double bond of C14=C27, it is expected that ring's electron density toraise.AIM analysis (Table **4**) shows that the ring's electron density (ρ(r)) will be increased from the amount of 0.047 a.u, in the structures I-a, I-b, I-c1 (I-c2),to the amount of 0.053 a.u, in the structures P-a, P-b andP-c1 (P-c2). The important point is that ring's electron density in all the intermediates and products were identical and independent of the substituted groups. The electronic charge of atoms C14, H15 and N28 in intermediate structures can play an important role in the proton transfer process. Although, there is no charge change in the proton donor atom (C14) and transferred atom (H15) in the structures ofI-a, I-b andI-c1 (I-c2), but the charge of the proton acceptor atom (N28) received some changes. Thus, it can influence the proton transfer process. Results show that due to the strict effect of the substituent groups and different electron transfers, the trend of charge change at the structures I-a, I-b andI-c1 (I-c2) is not equal to the structures of R1-a, R1-b, R1-c1 (R1-c2). Comparing with I-a, the charge of atom N28 increased at I-b and decreased at I-c1 (I-c2).The trend which was observed in the electronic charge of the atom N28in R1, was not observed in I. This can be due to various electron transfer, which has occurred as the result of the formation of C27-O9 and C27-C14 bonds. Proton transfer in the second step of the reaction had made unexpected changes in the atomic charge of the involved atoms. In the intermediate structures (I), atomic charge of the involved atom in the charge transfer process, are those that were expected. Minor changes in the atomic charge are due to the various substituent groups. In this structure, the atoms C14 and N28 have a negative charge and atom H15 has a positive charge. As expected, in the structure of the transition stateTS2, by approaching the atom H15 to atom N28, the negative charge of the atom N28 was increased and the positive charge of atom H15, because of approaching to an electronegative atom, was increased. As proton gets away from atom C14, electron density of atom C14 significantly decreased of the approximate -0.296e to 0.433e. In the structure of the product (P), the charge density of these atoms is different from those of intermediate structure (I) and transition state (TS2). Electron density of atom C14 will be increased, after formation of the C14-C27 double bond, so that it takes negative charge. Electron density change at the structures P-a, P-b andP-c1 (P-c2),unlike transition state and intermediate structures, is more significant. The atomic charge of N28 in the structure of P-a is -0.644e, while in P-b andP-c1 (P-c2) is0.352, 0.352, 0.379e, respectively. Also, the atomic charge of H15 in the structure of P-a is 0.389e, but in the structures of P-b, P-c1 (P-c2) is -0.224 and -0.224e (-0.185e), respectively. Results show that apart from the P-a structure, in other structures of P-b andP-c1 (P-c2), the manner is slightly unusual. The important electron transfer of LPN28→BD* C14-C27 in the structure of P-a is 29.21 kcal.mol-1, but this transmission in the structures of P-b andP-c1 (P-c2) is completely eliminated. This result was predictable, because of the positive charge concentration on N28 atom. In structure P-a, the LPN28→BD* C14-C27 electron transfer is in competition with LPN28→BD* O9-C27 one. In the structure I-a, these two electron transfer energy are2.67 and 24.34 kcal.mol-1, but in P-a are 29.21 and 1.85 kcal.mol-1and shows that increasing of the electron transfer energy of LPN28→BD* C14-C27 associated with decreasing the electron transfer energy of LPN28→BD* O9-C27. More detailed results revealed that the electron transfer of LPN28→BD* O9-C27 in the structures of P-b andP-c1 (P-c2) was also completely eliminate. This result was also expected based on the N28 atomic charge.

Table 3: NBO results including natural charges and charge transfer energies (E^2/kcal.mol^{-1}) in gas phase.

atom	charge	atom	charge	atom	charge	atom	charge
R1-a		**R2**		**TS1-a**		**TS1´-a**	
qC(27)	0.270	qC(7)	-0.217	qO(9)	-0.645	qO(9)	-0.646
qC(28)	-0.524	qC(8)	0.569	qC(27)	0.455	qC(27)	0.452
qC(29)	-0.209	qO(9)	-0.557	qC(28)	-0.402	qC(28)	-0.395
		qC(14)	-0.085	qC(29)	-0.204	qC(29)	-0.207
		qH(15)	0.229	CT	0.348	CT	0.353
LPC27→BD*N28-C29	17.04	LPO9→BD*C7-C8	21.83	LPO9→BD*C7-C8	18.43	LPO9→BD*C7-C8	18.57
		LPO9→BD*C7-C14	0.82	LPC27→BD*C7-C14	107.76	LPC7→BD*C8-O9	70.89
				LPC27→BD*N28-C29	11.04	LPC7→BD*C14-C27	83.39
LPC27→BD*N28-C29	17.04	LPO9→BD*C7-C8	21.83	LPO9→BD*C7-C8	18.43	LPO9→BD*C7-C8	18.57
I-a		**TS2-a**		**P-a**		**R1-b**	
qO(9)	-0.554	qO(9)	-0.525	qO(9)	-0.491	qC(27)	0.257
qC(14)	-0.296	qC(14)	0.421	qC(14)	-0.152	qC(28)	-0.527
qC(27)	0.622	qC(27)	0.382	qC(27)	0.514	qC(29)	-0.045
qC(28)	-0.486	qC(28)	-0.629	qC(28)	-0.644		
qC(29)	-0.217	qC(29)	-0.191	qC(29)	-0.186		
		qH(15)	0.446				
		CT	-0.037				
LPO9→BD*C7-C8	34.25	LPO9→BD*C14-C27	6.13	LPO9→BD*C7-C8	39.15	LPC27→BD*N28-C29	16.19
LPO9→BD*C27-N28	20.48	LPO9→BD*C27-N28	10.54	LPO9→BD*C14-C27	28.2		
LPN28→BD*O9-C27	24.34	LPN28→BD*O9-C27	11.35	LPN28→BD*O9-C27	1.85		
LPN28→BD*C14-C27	2.67			LPN28→BD*C14-C27	29.21		
TS1-b		**I-b**		**TS2-b**		**P-b**	
qO(9)	-0.629	qO(9)	-0.562	qO(9)	-0.532	qO(9)	-0.511
qC(14)	-0.092	qC(14)	-0.296	qC(14)	0.434	qC(14)	-0.021
qC(27)	0.452	qC(27)	0.620	qC(27)	0.559	qC(27)	-0.267
qC(28)	-0.420	qC(28)	-0.492	qC(28)	-0.642	qC(28)	0.352
qC(29)	0.098	qC(29)	0.091	qC(29)	0.107	qC(29)	0.053
LPC7→BD*C8-O9	74.38	LPO9→BD*C7-C8	32.05	LPO9→BD*C7-C8	24.96		
LPC7→BD*C14-C27	89.21	LPO9→BD*C27-N28	26.98	LPO9→BD*C27-N28	34.46		
LPO9→BD*C7-C8	19.87	LPN28→BD*O9-C27	29.69	LPN28→BD*O9-C27	13.96		
		LPN28→BD*C14-C27	3.54	LPN28→BD*C14-H15	74.59		
R1-c1		**TS1-c1**		**I-c1**		**TS2-c1**	
qC(27)	0.257	qO(9)	-0.636	qO(9)	-0.556	qO(9)	-0.531
qC(28)	-0.527	qC(14)	-0.087	qC(14)	-0.296	qC(14)	0.439
qC(29)	-0.045	qH(15)	0.258	qH(15)	0.252	qH(15)	0.429
		qC(27)	0.455	qC(27)	0.611	qC(27)	0.520
		qC(28)	-0.404	qC(28)	-0.477	qC(28)	-0.623
		qC(29)	-0.046	qC(29)	-0.047	qC(29)	-0.030
		CT	0.358			CT	0.123
		LPC7→BD*C8-O9	66.89	LPO9→BD*C7-C8	28.58	LPO9→BD*C27-N2**8**	12.68
		LPC7→BD*C14-C27	91.69	LPO9→BD*C27-N28	25.42	LPO9→BD*C28-C29	32.06
		LPO9→BD*C7-C8	18.67	LPN28→BD*O9-C27	26.51	LPN28→BD*O9-C27	13.15
P-c1		**R1-c2**		**TS1-c2**		**I-c2**	
qO(9)	-0.513	qC(29)	-0.043	qO(9)	-0.638	qO(9)	-0.557
qC(14)	0.013			qC(14)	-0.091	qC(14)	-0.296
qH(15)	-0.267			qH(15)	0.258	qH(15)	0.252
qC(27)	-0.203			qC(27)	0.453	qC(27)	0.612
qC(28)	0.381			qC(28)	-0.402	qC(28)	-0.478
qC(29)	-0.115			qC(29)	-0.044	qC(29)	-0.044
				CT	0.358		
		LPC7→BD*N28-C29	15.34	LPC7→BD*C14-C27	88.98	LPO9→BD*C7-C8	32.04
				LPO9→BD*C7-C8	18.69	LPO9→BD*C27-N2**8**	24.91
						LPN28→BD*O9-C27	27.08
TS2-c2		**P-c2**					
qO(9)	-0.531	qO(9)	-0.514				
qC(14)	0.438	qC(14)	0.017				
qH(15)	0.432	qH(15)	-0.273				
qC(27)	0.517	qC(27)	-0.185				
qC(28)	-0.626	qC(28)	0.379				
qC(29)	-0.030	qC(29)	-0.123				
CT	0.118						
LPO9→BD*C7-C8	3.26						
LPO9→BD*C27-N2**8**	15.22						
LPO9→BD*C14-C27	1.43						

Table 4: B3LYP/6-311++G(d,p)calculated topological properties of the BCPs (au) in all structures participated in the reaction mechanism.

structure	Bond	ρ(r)	∇^2 ρ(r)	G(r)	V(r)	H(r)	structure	Bond	ρ(r)	∇^2 ρ(r)	G(r)	V(r)	H(r)
R1-a	C27-N28	0.450	-0.318	0.744	-1.567	-0.823	**R1-c1**	C27-N28	0.450	-0.320	0.743	-1.566	-0.823
	N28-C29	0.260	-0.669	0.176	-0.518	-0.343		N28-C29	0.255	-0.638	0.175	-0.509	-0.334
R2	C7-C14	0.338	-1.025	0.128	-0.512	-0.384	**TS1-c1**	C7-C14	0.297	-0.786	0.095	-0.387	-0.292
	C14-H15	0.292	-1.101	0.036	-0.348	-0.312		C14-C27	0.086	0.051	0.039	-0.066	-0.027
TS1-a	C7-C14	0.297	-0.786	0.095	-0.387	-0.292		C27-N28	0.457	-0.196	0.790	-1.629	-0.839
	C14-C27	0.087	0.049	0.040	-0.067	-0.027		N28-C29	0.249	-0.551	0.197	-0.532	-0.335
	C27-N28	0.457	-0.213	0.785	-1.624	-0.839		C14-H15	0.300	-1.162	0.034	-0.358	-0.324
	N28-C29	0.250	-0.579	0.186	-0.517	-0.331							
TS1´-a	C7-C14	0.296	-0.780	0.094	-0.384	-0.289	**I-c1**	C7-C14	0.245	-0.519	0.060	-0.250	-0.190
	C14-C27	0.089	0.044	0.040	-0.069	-0.029		C14-C27	0.249	-0.552	0.059	-0.255	-0.197
	C27-N28	0.457	-0.220	0.784	-1.623	-0.839		C27-O9	0.263	-0.625	0.198	-0.551	-0.354
	N28-C29	0.248	-0.573	0.183	-0.510	-0.326		C27-N28	0.415	-1.281	0.365	-1.050	-0.685
I-a	C7-C14	0.245	-0.517	0.060	-0.249	-0.189		N28-C29	0.260	-0.653	0.107	-0.378	-0.271
	C14-C27	0.250	-0.557	0.059	-0.258	-0.198		C14-H15	0.286	-1.049	0.041	-0.344	-0.303
	C27-O9	0.267	-0.629	0.210	-0.578	-0.367		Ring	0.047	0.291	0.070	-0.068	0.003
	C27-N28	0.415	-1.289	0.363	-1.048	-0.685	**TS2-c1**	C7-C14	0.249	-0.524	0.070	-0.270	-0.201
	N28-C29	0.264	-0.665	0.105	-0.377	-0.271		C14-C27	0.298	-0.792	0.095	-0.389	-0.293
	C14-H15	0.286	-1.047	0.041	-0.343	-0.303		C27-O9	0.300	-0.672	0.289	-0.746	-0.457
	Ring	0.047	0.292	0.071	-0.068	0.003		C27-N28	0.374	-1.253	0.226	-0.765	-0.539
TS2-a	C7-C14	0.250	-0.527	0.070	-0.272	-0.202		N28-C29	0.256	-0.635	0.108	-0.375	-0.267
	C14-C27	0.297	-0.786	0.096	-0.388	-0.292		C14-H15	0.100	-0.036	0.040	-0.089	-0.049
	C27-O9	0.303	-0.679	0.294	-0.758	-0.464		N28-H15	0.125	-0.074	0.058	-0.135	-0.077
	C27-N28	0.374	-1.258	0.225	-0.764	-0.539		Ring	0.052	0.316	0.078	-0.076	0.001
	N28-C29	0.260	-0.653	0.107	-0.378	-0.271	**P-c1**	C7-C14	0.270	-0.629	0.080	-0.317	-0.237
	C14-H15	0.099	-0.031	0.040	-0.087	-0.048		C14-C27	0.330	-0.964	0.130	-0.501	-0.371
	N28-H15	0.128	-0.085	0.059	-0.139	-0.080		C27-O9	0.288	-0.520	0.305	-0.741	-0.435
	Ring	0.052	0.316	0.078	-0.076	0.001		C27-N28	0.318	-0.964	0.134	-0.508	-0.375
P-a	C7-C14	0.270	-0.629	0.079	-0.316	-0.237		N28-C29	0.253	-0.619	0.103	-0.360	-0.257
	C14-C27	0.331	-0.970	0.130	-0.502	-0.372		N28-H15	0.348	-1.702	0.061	-0.548	-0.487
	C27-O9	0.287	-0.513	0.305	-0.739	-0.434		Ring	0.053	0.343	0.083	-0.081	0.003
	C27-N28	0.317	-0.956	0.132	-0.504	-0.371	**R1-c2**	C27-N28	0.450	-2.971	0.743	-1.566	-0.823
	N28-C29	0.250	-0.585	0.098	-0.343	-0.245		N28-C29	0.254	-0.629	0.175	-0.508	-0.333
	N28-H15	0.349	-1.723	0.060	-0.551	-0.491	**TS1-c2**	C7-C14	0.296	-0.783	0.095	-0.385	-0.291
	Ring	0.053	0.344	0.083	-0.081	0.003		C14-C27	0.087	0.049	0.039	-0.067	-0.027
TS1-b	C7-C14	0.296	-0.783	0.095	-0.385	-0.290		C27-N28	0.457	-0.203	0.789	-1.629	-0.840
	C14-C27	0.087	0.049	0.039	-0.067	-0.027		N28-C29	0.248	-0.550	0.195	-0.527	-0.332
	C27-N28	0.457	-0.212	0.788	-1.629	-0.841		C14-H15	0.300	-1.165	0.034	-0.359	-0.325
	N28-C29	0.241	-0.545	0.176	-0.488	-0.312	**I-c2**	C7-C14	0.245	-0.519	0.060	-0.250	-0.190
I-b	C7-C14	0.246	-0.522	0.060	-0.251	-0.191		C14-C27	0.249	-0.552	0.059	-0.256	-0.197
	C14-C27	0.248	-0.545	0.058	-0.253	-0.195		C27-O9	0.263	-0.624	0.198	-0.551	-0.354
	C27-O9	0.261	-0.620	0.193	-0.541	-0.348		C27-N28	0.415	-1.283	0.365	-1.051	-0.686
	C27-N28	0.415	-1.261	0.372	-1.058	-0.687		N28-C29	0.260	-0.653	0.107	-0.377	-0.270
	N28-C29	0.251	-0.604	0.100	-0.351	-0.251		C14-H15	0.286	-1.049	0.041	-0.344	-0.303
	C14-H15	0.280	-1.003	0.043	-0.337	-0.294		Ring	0.047	0.291	0.070	-0.068	0.003
	Ring	0.047	0.291	0.070	-0.067	0.003	**TS2-c2**	C7-C14	0.249	-0.524	0.070	-0.271	-0.201
TS2-b	C7-C14	0.250	-0.527	0.070	-0.272	-0.202		C14-C27	0.298	-0.792	0.095	-0.389	-0.293
	C14-C27	0.297	-0.787	0.095	-0.387	-0.292		C27-O9	0.300	-0.672	0.289	-0.745	-0.457
	C27-O9	0.299	-0.670	0.287	-0.742	-0.455		C27-N28	0.374	-1.256	0.226	-0.766	-0.540
	C27-N28	0.372	-1.238	0.221	-0.751	-0.530		N28-C29	0.256	-0.633	0.107	-0.373	-0.266
	N28-C29	0.248	-0.584	0.100	-0.347	-0.246		C14-H15	0.100	-0.035	0.040	-0.089	-0.049
	C14-H15	0.102	-0.041	0.041	-0.091	-0.051		N28-H15	0.126	-0.075	0.058	-0.136	-0.077
	N28-H15	0.125	-0.070	0.059	-0.135	-0.076		Ring	0.052	0.316	0.078	-0.076	0.001
	Ring	0.052	0.316	0.077	-0.076	0.002	**P-c2**	C7-C14	0.270	-0.628	0.079	-0.316	-0.237
P-b	C7-C14	0.271	-0.633	0.080	-0.318	-0.238		C14-C27	0.330	-0.962	0.129	-0.500	-0.370
	C14-C27	0.330	-0.964	0.129	-0.498	-0.370		C27-O9	0.288	-0.521	0.305	-0.741	-0.436
	C27-O9	0.285	-0.513	0.301	-0.730	-0.429		C27-N28	0.319	-0.967	0.134	-0.510	-0.376
	C27-N28	0.317	-0.947	0.132	-0.500	-0.368		N28-C29	0.253	-0.619	0.103	-0.361	-0.258
	N28-C29	0.242	-0.548	0.093	-0.323	-0.230		N28-H15	0.348	-1.708	0.061	-0.549	-0.488
	N28-H15	0.349	-1.708	0.062	-0.551	-0.489		Ring	0.053	0.343	0.083	-0.081	0.003
	Ring	0.053	0.344	0.083	-0.081	0.003							

3.3. Nuclear Magnetic Resonance (NMR)

To analyze the optimized structure of the product, NMR calculation was performed on various structures of final products. The most rational structures were identified based on the experimental NMR analysis. The amount of atom's chemical shift in products related to the calculated and the experimental amounts is depicted in Table **5**. Results show a logical match between experimental and theoretical results. Rotation of the C27-N28 bond in all products (P), a new configuration is expected to be exist. More detailed investigations on the one of these structures (P'-b)(Fig. 2) showed that the structure P-b, with having more thermodynamic stability (-94.73)compared to P′-b (-89.67), shows thermodynamic preference. It is not reasonable that the reaction with an additional step goes towards a more stable product.

Table 5: Selected ^{1}H NMR chemical shift (δ) for some functional groups in **P-a ،P-b ،P'-b ،P-c1**and**P-c2** structures.

groups	δ^{H}/ppm	groups	δ^{H}/ppm
P-a		**P-b**	
6H, 2s, 2 CH_3	1.62 (2.75) 2.13 (3.17)	9H, s, CMe_3	1.60 (1.72)
1H, br s, N-H	3.58 (3.69)	3H , s, CH_3	2.15 (3.07)
2H, CH_2	4.76 (5.26) 4.54 (4.40)	3H , s, CH_3	1.85 (2.73)
10H, m, $2C_6H_5$	7.1-7.5 (7.81)	1H, br s, N-H	3.9 (3.51)
		5H, m, C_6H_5	7.2-7.5 (7.95)
P-b´		**P-c1**	
9H, s, CMe_3	1.60 (1.30)	10H, m, $5CH_2$	1.2-2.3 (2.03)
3H , s, CH_3	2.15 (3.06)	3H , s, CH_3	2.15 (3.06)
3H , s, CH_3	1.85 (2.78)	3H , s, CH_3	1.78 (2.73)
1H, br s, N-H	3.9 (2.45)	1H, t, , 2.7 HZ, CH-N	3.41 (4.25)
5H, m, C_6H_5	7.2-7.5 (7.94)	1H, br s, N-H	3.60 (3.27)
		5H, m, C_6H_5	7.2-7.5 (7.94)
P-c2		**P-c2**	
10H, m, $5CH_2$	1.2-2.3 (1.96)	1H, tt, 2.7 HZ, CH-N	3.41 (3.91)
3H , s, CH_3	1.78 (2.73)	1H, br s, N-H	3.60 (3.46)
3H , s, CH_3	2.15 (3.05)		

Also, NMR data revealed that due to the vicinity of H15 to O6 in the structure of **P′-b**, the chemical shift of this atom transferred to the lower fields, compared to **P-b** and its deviance from experimental amount has increased. Therefore, NMR analysis also won't confirm the formation of such products.

Rate Equation

The obtained results from quantum calculations in gas phase and in the presence of different solvents (acetone and dichloromethane) and also in the presence of different substituted groups illustrate that the second energy barrier is significantly higher than the first energy barrier and was found as rate-determining step. Rewriting the rate equation for ultimate product and replacement of values for intermediate concentrations in this equation and based on equation (1), a final equation for the given reaction is obtained. The rate constant is of the second order due to the bimolecular transition state in the first step of the reaction.

$$\begin{aligned} R1 + R2 &\underset{k_{-1}}{\overset{k_1}{\rightleftharpoons}} I \\ I &\xrightarrow{k_2} P \end{aligned} \qquad (1)$$

The reaction rate can be express as:

$$rate = k_2[I] \qquad (2)$$

By applying the rate-determining step approximation;

$$[I] = \frac{k_1}{k_{-1}}[R1][R2] \qquad (3)$$

Inserting in equation (3) into equation (2) we have:

$$rate = k[R1][R2] \quad , \quad k = \frac{k_1 k_2}{k_{-1}} \qquad (4)$$

The final rate equation shows that the total rate constant of the reaction will be the second order which depends on the R1 and R2 concentration.

Conclusions

Quantum mechanical calculations were made in order to study the potential energy surfaces, energetic, vibrational frequencies and topological properties of all structures in the reaction of alkyl isocyanides (contains methyl benzene isocyanide, tert-butyl isocyanide, cyclo hexyl socyanide) with 3-Benzylidene-2,4-pentanedione in gas phase and in different solvents such as acetone and dichloromethane. The results can be summarized as follows:

1. Contrary to what was expected, in each reaction path, the second step of the reaction which contains an intermolecular proton transfer, recognized as rate-determining step.
2. In dichloromethane and acetone solvents, no especial difference in the energy barrier of the first and the second step of the reaction was observed. All the structures in acetone solvent had been more stable compared to dichloromethane. Results show that the amount of change in potential energy surfaces in both acetone and dichloromethane solvents with different dielectric constants was approximately equal.
3. The energy level of the most stable product in the presence of both solvents and in gas phase corresponds to P-a and the path a was determined as thermodynamically stable path. The least barrier height corresponds to the path band determined as a kinetically stable path.
4. Results show that in going fromR1-a to R1-b or R1-c1 (R1-c2), increasing of the negative chargeof N28 and decreasing of the positive charge of C27 is the result of increasing electron donation of substituted groups of t-butyl or cyclohexyl.
5. The high energy barrier of the two reaction steps well shows why the reaction doesn't proceed at room temperature.

Computational details

In this work, we studied the effect of the adsorption of gas molecules (H_2O and HF) on the surface of PCNTs and ZnGa-doped CNT by using the density functional theory (DFT) calculations, as well as structural and electronic properties including bond lengths, bond angles, energy gaps, molecular orbital energies, adsorption energy and total energy. Our results suggest that the ZnGa-doped CNT are more favorable than PCNT models for gases adsorption due to large adsorption energy (E_{ad}) at doping. Thus can be used to design nanostructure as chemical sensors, and PCNTs and ZnGa-doped CNT could be used to build sensors for the detection to purify the air of pollutants. Where we doping carbon nanotubes with zinc and gallium atoms with the doping ratio reached 1.6 % as shown in Figs. 2. The adsorption energy (E_{ads}) of (HF and H_2O) molecules on the pristine and ZnGa-doped CNT was calculated as follows:

$$E_{ad\ (pristine\ system\ )} = E_{(pristine\ system)} - (E_{\ CNT} + E_{gas}) \quad \ldots\ldots\ (1)$$

$$E_{ad\ (doping\ system)} = E_{(doping\ system)} - (E_{\ ZnGa\text{-}CNT} + E_{gas}) \quad \ldots\ldots\ (2)$$

Where: $E_{(pristine\ system)}$ and $E_{\ (doping\ system)}$ represent total energies of the gas molecules on the CNT and ZnGa-CNT respectively , E_{CNT} and $E_{ZnGa\text{-}CNT}$ represent the energies of the isolated CNT and ZnGa-CNT and E_{gas} is the energy of the isolated gas molecule. The diversity of relative energy of the highest occupied (HOMO) and the lowest unoccupied molecular orbital (LUMO) of free ZnGa-CNT and adsorbed molecule on ZnGa-CNT demonstrated the mechanism of interaction[20].

Acknowledgements

Authors sincerely thank the Payam Noor University for providing financial support of this work.

References

[1] Zangouei, M.; Esmaeili, A. A.; Habibi, A.; Fakhari, A. R. *Tetrahedron*. **2014**, *70*, 8619.
[2] Banfi, L.; Basso, A.; Guanti, G.; Lecinska, P.; Riva, R. *Mol. Diversity*. **2008**, *12*, 187.
[3] Wang, J.; Sun, Y.; Wang, G.; Zhen, L. *Eur. J. Org. Chem.* **2017**, *2017*, 6338.
[4] Adib, M.; Sheikhi, E.; Azimzadeh, M. *Tetrahedron Lett.* **2016**, *56*, 1933.
[5] Khan, M. W.; Alam, M. J.; Rashid, M. A. *Med Chem.* **2005**, *13*, 4796.
[6] Baharfar, R.; Baghbanian, S. M. *Chin. Chem. Lett.* **2012**, *23*, 677.
[7] Yeung, K. S.; Yang, N.; Peng, X. S.; Hou, X. L. *Prog. Heterocycl. Chem.* **2011**, *22*, 181.
[8] Cho, C. H.; Larock, R. C. *ACS Comb. Sci.* **2011**, *13*, 272.
[9] Haines, N. R.; VanZanten, A. N.; Cuneo, A. A.; Miller, J. R.; Andrews, W. J.; Carlson, D. A.; Harrington, R. M.; Kiefer, A. M.; Mason, J. D.; Pigza, J. A.; Murphree, S. S. *J. Org. Chem.* **2011**, *76*, 8131.

[10] Yoshimura, F.; Sasaki, M.; Hattori, I.; Komatsu, K.; Sakai, M.; Tanino, K.; Miyashita, M. *Chem. Eur. J.* **2009**, *15*, 6626.
[11] Lee, H. K.; Chan, K. F.; Hui, C. W.; Yim, H.K.; Wu, X. W.; Wong, N. C. *Pure. Appl. Chem.* **2005**, *77*, 139
[12] Montagnon, T.; Tof, M.; Vassilikogiannakis, G. *Acc. Chem. Res.* **2008**, *41*, 1001.
[13] Gandini, A.; Silvestre, A. J. D.; Neto, C.P.; Sousa, F. A.; Gomes, M. *J. Polym. Sci.* **2009**, *47*, 295.
[14] Murphy, E. B.; Wudl, F. *Prog. Polym. Sci.* **2010**, *35*, 223.
[15] Peart, P. A.; Tovar, J. D. *Macromolecules*. **2009**, *42*, 4449.
[16] Umeyama, T.; Takamatsu, T.; Tezuka, N.; Matano, Y.; Araki, Y.; Wada, T.; Yoshikawa, O.; Sagawa, T.; Yoshikawa, S.; Imahori, H. *J. Phys. Chem. C.* **2009**, *113*, 10798.
[17] Wong, H. N. C.; Hou, X. L.; Yeung, K. S.; Huang, H.; Alvarez-Builla, J.; Vaquero, J. J. *Five-Membered Heterocycles: Furan;* Wiley-VCH Weinheim: Germany, **2011**.
[18] Sarvary, A.; Shaabani, S.; Shaabani, A. *Tetrahedron*. **2011**, *67*, 3624.
[19] Yavari, I.; Shaabani, A.; Maghsoodlou, M. T. *Month. Chem.* **1997**, *128*, 697.
[20] Frisch, M. J.; Trucks, G. W.; Schlegel, H. B.; Scuseria, G. E.; Robb, M. A.; Cheeseman, J. R.; Scalmani, G.; Barone, V.; Mennucci, B.; Petersson, G. A.; Nakatsuji, H.; Caricato,M.; Li, X.; Hratchian, H. P.; Izmaylov, A. F.; Bloino, J.; Zheng, G.; Sonnenberg, J. L.; Hada, M.; Ehara, M.; Toyota, K.; Fukuda, R.; Hasegawa, J.; Ishida, M.; Nakajima, T.; Honda, Y.; Kitao, O.; Nakai, H.; Vreven, T.;Montgomery, J. A. Jr.; Peralta, J. E.; Ogliaro, F.; Bearpark, M.; Heyd, J. J.; Brothers, E.; Kudin, K.N.; Staroverov,V.N.; Kobayashi, R.;Normand, J.; Raghavachari,K.; Rendell, A.; Burant, J.C.; Iyengar, S. S.; Tomasi, J.;Cossi,M.; Rega,N.; Millam, J. M.; Klene,M.; Knox, J. E.; Cross, J. B.; Bakken, V.; Adamo, C.; Jaramillo, J.;Gomperts, R.; Stratmann, R. E.; Yazyev,O.; Austin,A. J.; Cammi, R.; Pomelli, C.; Ochterski, J. W.; Martin, R. L.; Morokuma, K.; Zakrzewski, V. G.; Voth, G. A.; Salvador, P.; Dannenberg, J. J.; Dapprich, S.; Daniels, A. D.; Farkas, O.; Foresman, J. B.; Ortiz, J. V.; Cioslowski, J.; Fox,D. J. Gaussian 09.Gaussian Inc.:Wallingford, **2009**.
[21] Schmidt, M.W.; Baldridge, K. K.; Boatz, J. A.; Elbert, S. T.; Gordon, M. S.; Jensen, S. H.; Koseki, S.; Matsunaga, N.; Nguyen, K. A.; Su, S.; Windus, T. L.; Dupuis, M. Montgomery, J. A. *J. Comput. Chem.* **1993**, *14*, 1347.
[22] Gonzalez, G.; Schlegel, H.B. *J. Phys. Chem.* **1990**, *94*, 5523.
[23] Gonzalez, C.; Schlegel H. B. *J. Chem. Phys.* **1989**, *90*, 2154.
[24] Fukui, K. *J. Phys. Chem.* **1970**, *74*, 4161.
[25] Fukui, K. *Acc. Chem. Res.* **1981**, *14*, 363.
[26] Tomasi, J.; Persico, M. *Chem. Rev.* **1994**, *94*, 2027.
[27] Cances, E.; Mennucci, B.; Tomasi, J. *J. Chem. Phys.* **1997**, *107*, 3032.
[28] Cossi, M.; Barone, V.; Cammi, R. *J. Chem. Phys. Lett.* **1996**, *255*, 327.
[29] Glendening, D. E.; Reed, A. E.; Carpenter, J. E.; Weinhold, F. NBO, **2009**, Version 3.1.
[30] Biegler-Knig, F.; Schnbohm, J.; Bayles, D. *J. Comput. Chem.* **2001**, *22*, 545.